

# LONGITUDINAL BEAM DIAGNOSTICS FOR THE ILC INJECTORS AND BUNCH COMPRESSORS\*

P. Piot<sup>1,4</sup>, A. Bracke<sup>1</sup>, V. Demir<sup>2</sup>, C. Jing<sup>3</sup>, T. Maxwell<sup>1,4</sup>, J. G. Power<sup>3</sup>, M. M. Rihaoui<sup>1,3</sup>

<sup>1</sup> Department of Physics, Northern Illinois University DeKalb, IL 60115

<sup>2</sup> Department of Electrical Engineering, Northern Illinois University DeKalb, IL 60115

<sup>3</sup> High Energy Physics Division, Argonne National Laboratory, Argonne, IL 60439, USA

<sup>4</sup> Accelerator Physics Center, Fermi National Accelerator Laboratory, Batavia, IL 60510, USA

## Abstract

We present a diagnostics suite and analyze techniques for setting up the longitudinal beam dynamics in International Linear Collider e- injectors and e+ and e- bunch compressors. Techniques to measure the first order moments and recover the first order longitudinal transfer map of the injector's intricate bunching scheme are presented. Coherent transition radiation diagnostics needed to measure and monitor the bunch length downstream of the  $\sim 5$  GeV bunch compressor are investigated using a vector diffraction model.

## INTRODUCTION

In the foreseen International Linear Collider (ILC) electron and positron bunches are collided at 500 GeV in the center-of-mass. The design luminosity requires the bunches to be as short as  $100 \mu\text{m}$  (rms) at the interaction point [1]. A bunch compressor based on a two-stage wiggler scheme is used to compress the bunch by a factor  $\sim 30$  to 50 at  $\sim 5$  GeV downstream of the damping ring before entering the main linac [2].

Before injection in the damping ring both electron and positron beams undergo intricate longitudinal phase space manipulation. The electron beam is generated via photoemission using a long laser pulse to mitigate space charge. The beam bunching is then done via ballistic bunching using sub-harmonic bunchers. After acceleration to 5 GeV, the beam is then manipulated to reduce its fractional energy spread in a so-called energy compressor to satisfy the damping ring requirements. The positron beam is manipulated in similar ways but its low energy dynamics is more intricate due to the transverse-longitudinal coupling imparted in the capture and adiabatic matching section which is optimized to collect and the positrons downstream of the convertor.

In this paper we give an overview of our effort to develop several longitudinal phase space diagnostic systems and techniques to monitor the longitudinal phase space gymnastics along the ILC injectors and bunch compressors.

Numerical simulations, hardware development along with experimental tests are discussed. The goal of this work is to ultimately provide technique for setting-up and monitoring the main components of ILC bunching systems.

## LONGITUDINAL TRANSFER MAP FUNCTIONS

### Concept

The measurement of longitudinal transfer function (LTF) consists of impressing a perturbation (e.g. photocathode drive-laser phase shift, phase or amplitude variation of a rf cavity) around its nominal operating point and measuring the associated effect on the time-of-flight (TOF) of the electron (or positron) bunch using phase detectors and energy measurements located downstream. This method was pioneered in the CEBAF recirculating accelerator at Jefferson Lab [3] and later implemented in an energy recovering free-electron laser [4]. Depending on the type of perturbation (phase or amplitude) and the corresponding measurement (TOF or energy change), one can in principle access to all the element of the longitudinal phase space transfer map. For instance varying phase of a cavity and measuring the associated TOF (resp. energy) variation provide information on the  $\langle t|t \rangle$  [resp.  $\langle E|t \rangle$ ] elements whose first order expansions under TRANSPORT formalism are the transfer matrix elements  $M_{55}$  (resp.  $M_{65}$ ).

The LTF technique is in principle applicable in both electron and positron injectors. In the case of the positron injector, the impact on the diagnostics of the intricate coupling between longitudinal and transverse dynamics (in the adiabatic matching section) remains to be studied. Simulations of the ILC electron injector proposed in Ref. [5] were performed to investigate the possible use of LTF as a way to set-up the bunching system in the electron injector: an example of simulated compression efficiency ( $\langle t|t \rangle$ ) patterns is presented in Fig. 1 for the nominal setting of the bunching setting, and for two cases of mis-tuning of the injector sub-harmonic buncher. It is seen that different parameters affect the LTF in different ways. Here the photocathode laser phase is varied and the phase corresponding relative TOF change is recorded downstream of the pre-accelerator at about  $\sim 60$  MeV. The simulation we carried with ASTRA [6]. The observed changes in the LTF pattern depend-

\*This work is supported by the U.S. D.O.E. under Contract DE-FG02-06ER41435 with Northern Illinois University and under Contract No. DE-AC02-06CH11357 with Argonne National Laboratory. The work of P.P. and T. M. is partially sponsored by the Fermi Research Alliance, LLC under Contract No. DE-AC02-07CH11359 with the U.S. D.O.E.

ing upon the sub-harmonic buncher demonstrates the usefulness of the technique for troubleshooting the longitudinal phase space manipulation in the ILC injectors.

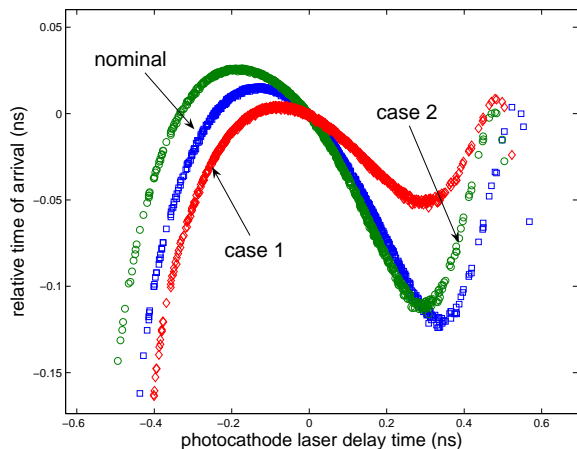


Figure 1: An example of the sensitivity of longitudinal transfer function (LTF) on the bunching system of the electron injector for the nominal setting, the case when the first subharmonic buncher amplitude is detuned by 20% (case 1) and the case when the second sub-harmonic bunch phase is changed by  $-20^\circ$  (case 2). In these simulations, the photocathode drive-laser phase was varied and the corresponding time-of-flight from the photocathode to the diagnostics located downstream of the bunching section was measured.

Similar results have been obtained for the ILC bunch compressor. Single-particle beam dynamics simulations of the baseline detailed in Ref. [2] were performed using a one-dimensional program [7]. We modeled the LTF measurement by considering two phase detectors located downstream of each of the wiggler chicanes composing the bunch compressor. A possible measurement would consist in varying the phase of the two linac sections in the bunch compressor: this would be equivalent to a change in incoming bunch arrival time. The measurements of the relative change of TOF downstream of each of the chicanes provide information on the associated  $\langle t|t \rangle$  LTF. We performed simulations for several tunes of the first bunch compressor linac phase; see Fig. 2. The simulations also include the phase and relative amplitude jitter of the bunch compressor linacs [taken to be respectively  $0.25^\circ$  (rms) and  $1 \times 10^{-3}$  (rms)]. Although the inclusion of the linac jitter sources greatly reduce the sensitivity of the measured LTF on mis-settings of the phase of the first linac section, the technique still provides sufficient information for troubleshooting purposes.

### Implementation & preliminary tests

In view of the relatively large bunch length compared to, e.g., FEL accelerators, the required sensitivity for the time-of-flight detector is in the 100 fs regime. Such a resolution can be achieved using conventional rf mixing tech-

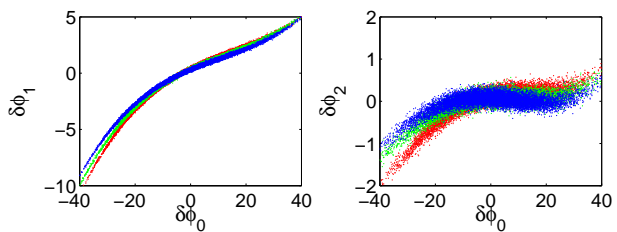


Figure 2: An example of the sensitivity of longitudinal transfer function (LTF) of the bunch compressor system for the nominal setting (red), and a change in  $\pm 2^\circ$  in the phase of the first stage bunch compressor linac. In these simulations, the incoming bunch arrival time (phase  $\delta\phi_0$ ) and the thereby induced phase shift downstream of the first stage ( $\delta\phi_1$ ) and second stage ( $\delta\phi_2$ ) of the bunch compressor is recorded.

niques [9]. The phase detector schematics is presented in Fig. 3. The signals generated by the four electrodes of a 1.3 GHz stripline beam position monitor (BPM) are filtered using a 1.3 GHz waveguide-style bandpass filters bandpass filter (BPF) and sent to a rf printed circuit board designed with the method of moment technique [10]. Inside the board the four input signals are coupled and combined to minimize position dependence. The 1.3 GHz reference signal with variable phase is also sent to the circuit. The circuit uses an Analogue Device phase comparator to provide the phase difference between the beam-induced signal and the reference. Part of the combined rf signal is coupled out before being sent to the phase comparison so it could be fed into another phase monitor as reference signal for a phase comparison between phase monitor.

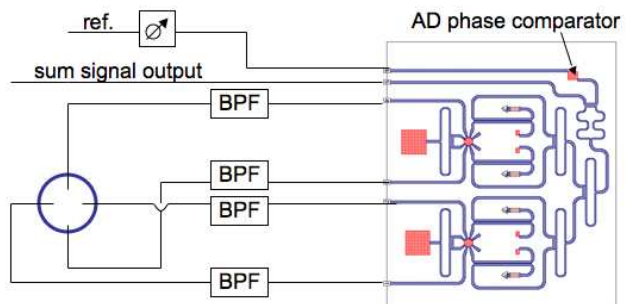


Figure 3: Block diagram of the phase detector assembly. The four signals from a beam position monitor (BPM) are filtered with 1.3 GHz band pass filter (BPM) and compared with the reference signal to yield the phase. The sum/comparison is performed in a rf board.

Preliminary tests were performed at the Argonne Wakefield Accelerator [11]. For these tests the beam-induced signal from a 2.856 GHz stripline antenna was filtered in a 1.3 GHz band pass filter [12] and sent to an Analogue Device phase comparator chip together with a phase-shiftable

copy of the reference signal from the master oscillator. The charge during these experiments was approximately 1 nC and the resulting signals are shown in Fig. 4. The signal was sensitive to the accelerator settings, e.g. rf gun phase, but large phase jitter noise prevented a clean measurement of the LTF. This will be performed in the near future.

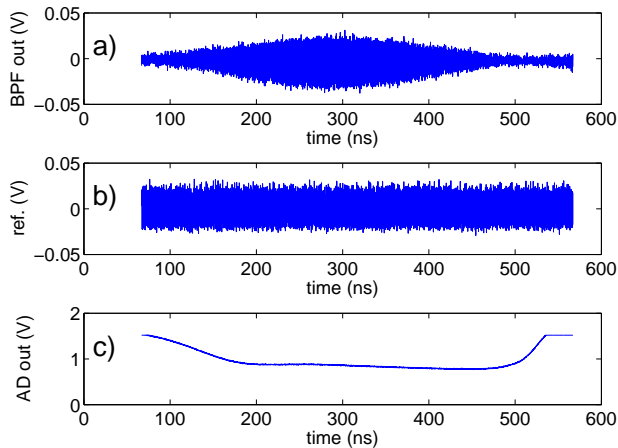


Figure 4: Preliminary test of the phase detector at the AWA. The beam induced signal downstream of the 1.3 GHz BPF (a) is compared to the 1.3 GHz reference signal (b) in a Analogue Device chip whose output (c) is proportional to the phase shift between the beam-induced and reference signals.

## COHERENT TRANSITION RADIATION

Frequency-domain analysis of radiation produced by relativistic picosecond-long electron beam can provide information on the beam’s charge density. In particular interferometry and spectrometry of coherent transition radiation (TR) emitted by the bunch have proved to be powerful diagnostics. However, for the range of bunch length expected downstream of the ILC bunch compressors ( $\sigma_z \in [150 - 500] \mu\text{m}$  depending on the mode of operation; see Ref. [1]), the relevant wavelength range of the coherent radiation is in the sub-millimeter regime, a regime where diffraction effects significantly alter the response function of the bunch length diagnostics based on coherent radiation. In the case of coherent transition radiation, for instance, the finite diameter of the metallic foil used as a radiator will affect the spectrum of the sub-mm wavelength TR. Another noxious effect results from the high energy which force to locate the detector in the near field region [i.e. the observation point  $R$  is at a distance much smaller than the “formation length” associated to transition radiation  $R < \gamma\lambda^2$ , where  $\gamma$  is the Lorentz factor and  $\lambda$  the observation wavelength]. Both of these effects preclude the use of the Frank-Ginzburg formula. A software based on wavefront propagation was developed and used to model the generation and transport of TR [13]. An example of calculation performed for a 5 GeV electron striking a finite

size TR radiator is depicted in Fig. 5 showing the frequency response of a TR-based diagnostics. An algorithm to correct for this non-uniform response have been developed and numerically tested [14]. Simulations spectral analysis via dispersion through a grating have also been performed [15].

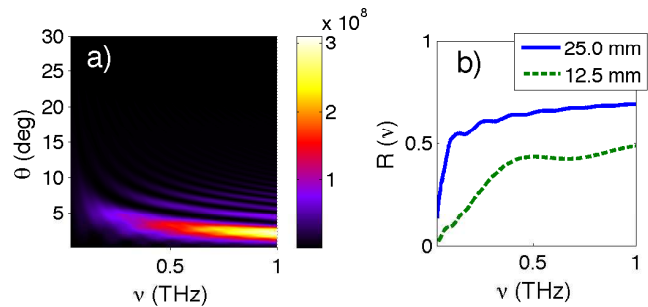


Figure 5: Transition radiation generated by a 5 GeV electron in the sub-mm wavelength regime. Left plot: spectral spectral radiance with a 25 mm foil at observation distance  $R = 15.24 \text{ cm}$  ( $\simeq 6''$ ). Right plot: acceptance ratios  $R(\nu)$  of viewing windows of 12.5 mm and 25.0 mm radius at a distance of 15.2 cm from the emission source.

## REFERENCES

- [1] See T. Raubenheimer, ”Suggested beam parameters for ILC”, available at <http://www-project.slac.stanford.edu/ilc/acceldev/beampar/>.
- [2] S. Seletskiy, P. Tennenbaum, in Proc. PAC07 (Albuquerque), 1958 (2007)
- [3] G. A. Krafft, in AIP Conf. Proc. **367**, 46 (1996).
- [4] P. Piot, *et al.*, *PRSTAB* **6**, 030702 (2003).
- [5] A. Curtoni, M. Jablonka, report TESLA-2001-22 available from DESY (2001).
- [6] K. Flöttmann, ASTRA: A Space Charge Tracking Algorithm, available at <http://www.desy.de/~mpyflo>.
- [7] P. Piot, Fermilab report Beams Document 3335-v1 (2009).
- [8] D. Hardy, *et al.*, in Proc of PAC97, 2265 (2007).
- [9] N. S. Sereno, *et al.*, *PRSTAB* **11**, 072801 (2008).
- [10] M. H. Al Sharkawy, V. Demir, A. Z. Elsherbeni, *Electromagnetic Scattering using the iterative multi-region Technique*, Synthesis Lecture on Computational Electromagnetics, Morgan & Claypool Publishers, December 2007.
- [11] See for information <http://www.hep.anl.gov/awa/>.
- [12] The waveguide-type bandpass filter was designed by the Microwave Filter Company, Inc.
- [13] T. J. Maxwell *Diffraction Analysis of Coherent Transition Radiation Interferometry in Electron Linear Accelerators*, Master of Science Thesis, Northern Illinois University (2007).
- [14] T. J. Maxwell *et al.*, in Proc. of BIW08 (Lake Tahoe) paper # TUPTPF020 (in press, 2008).
- [15] T. J. Maxwell *et al.*, manuscript in preparation.